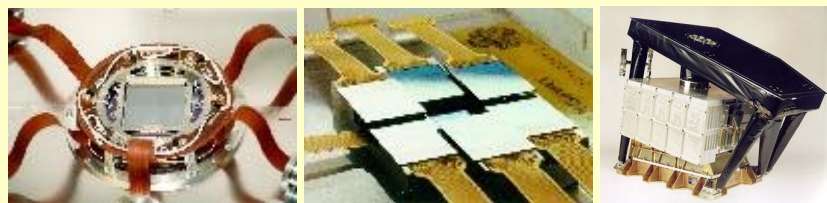




Update on the status of the XMM-Newton calibrations



IACHEC Meeting, Ringberg Schloss
19 May 2008

Matteo Guainazzi, Andy Pollock, Martin
Stuhlinger, Richard Saxton, Marcus Kirsch

with inputs of the whole EPIC and RGS consortia



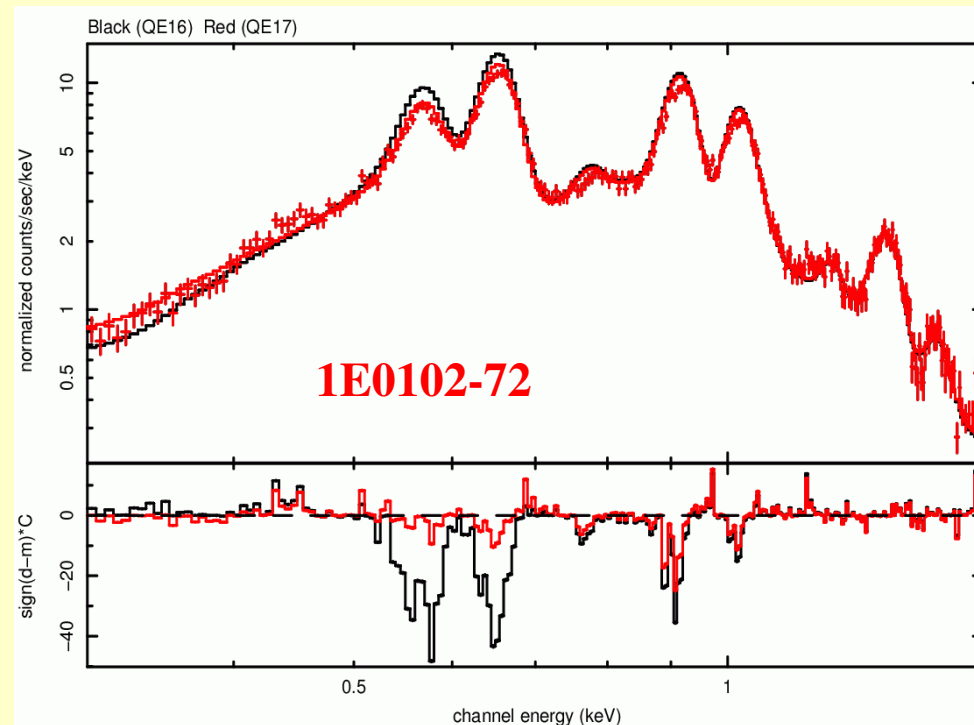
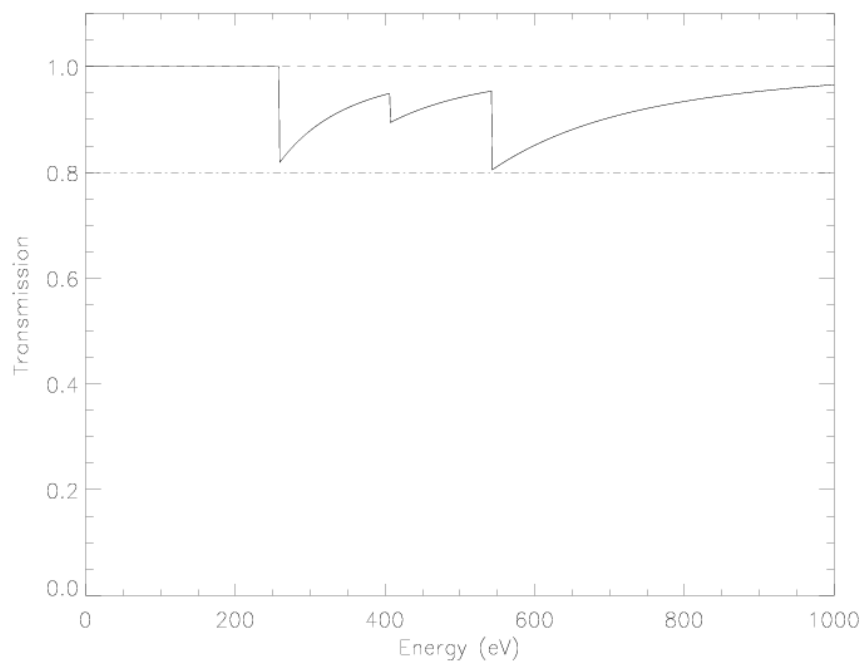
Outline

- Effective area improvements
 - MOS QE refinement
 - pn gain/CTI refinement
 - RGS effective area correction
 - RGS long-term contamination correction
- Status of cross-calibration among the XMM-Newton X-ray cameras
- The XMM-Newton SOC cross-calibration archive:
 - XMM-Newton vs. *Chandra*
 - XMM-Newton vs. *Suzaku*



MOS QE

Adjustment of the MOS Quantum Efficiency at the C, N, O edges



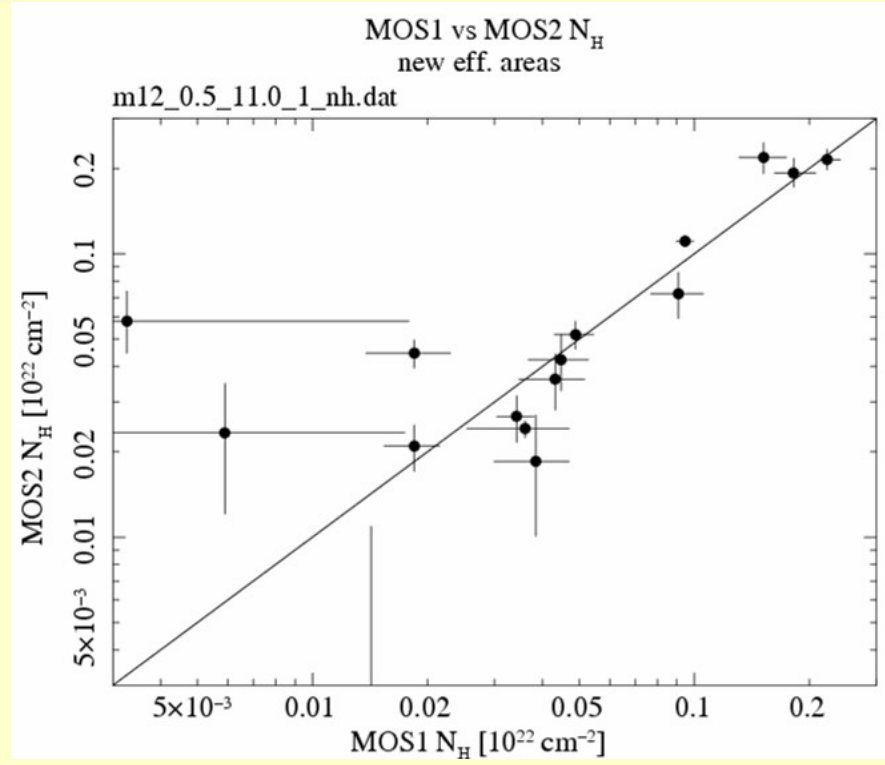
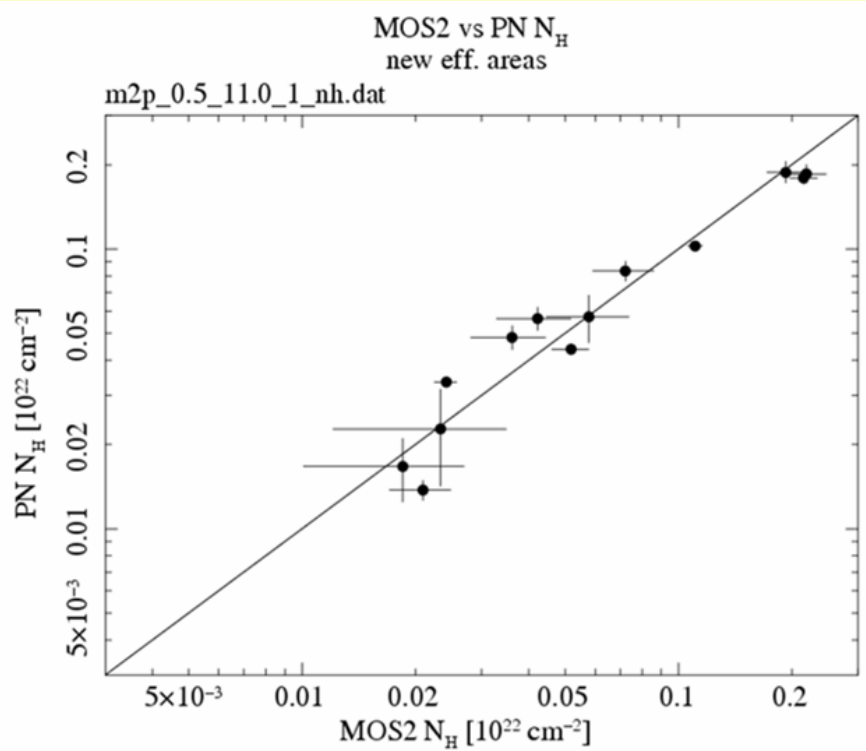
(Sembay 2007)

Impact:

- Significant improvement at the Oxygen lines once compared with models based on high-resolution (RGS, HETG) data
- Better pn-MOS imaging mode cross-calibration



EPIC N_H comparison for 21 blazars



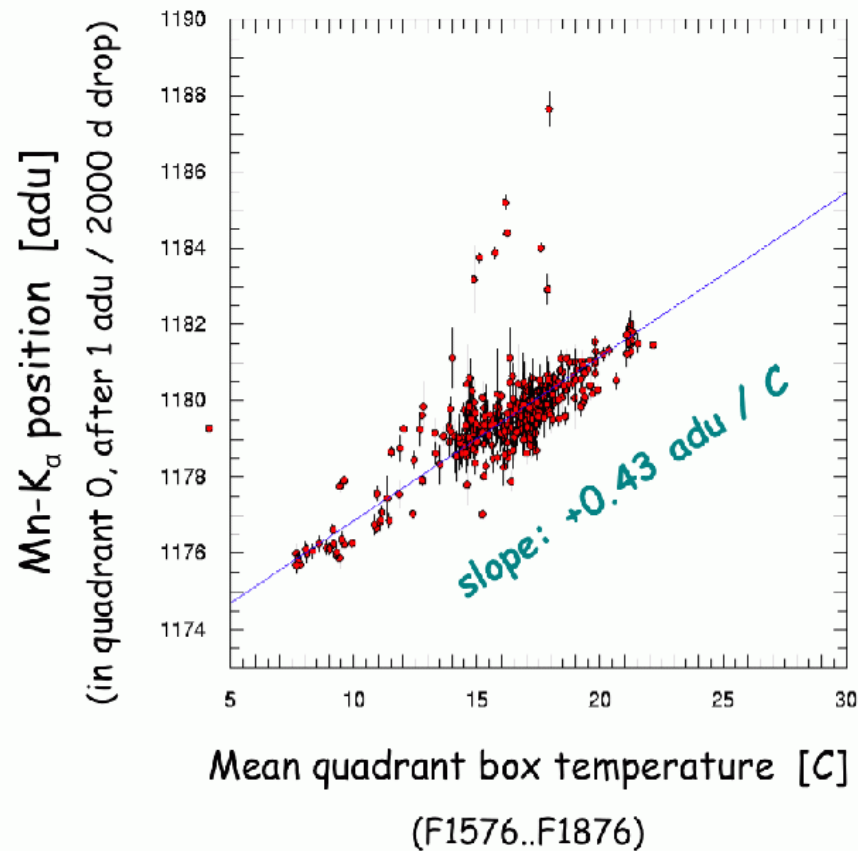
(Molendi, 2007)

After QE update:

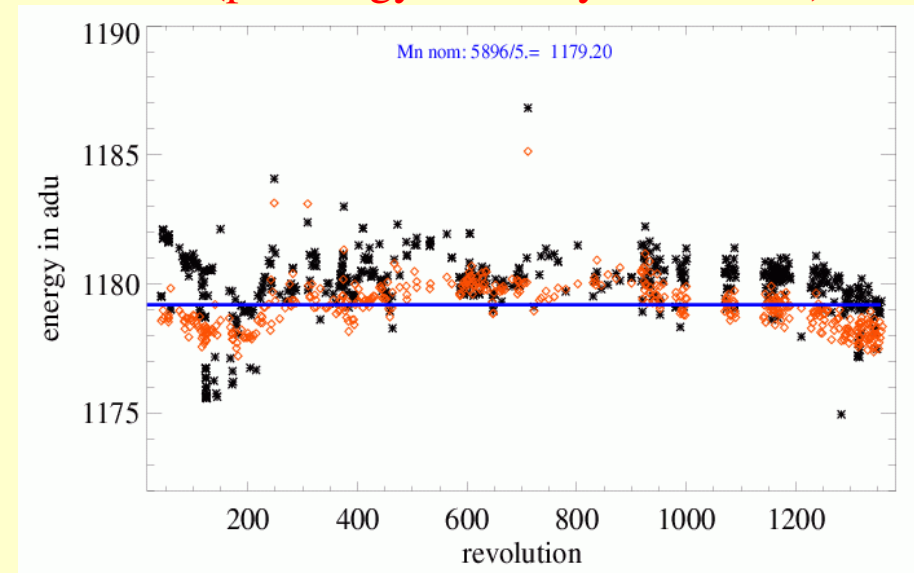
- Very good agreement between MOS and pn
- Agreement between MOS1 and MOS2 remains good



pn FF gain temperature-dependence



Without temperature correction
With temperature correction
(pn energy accuracy $\leq 5-10$ eV)



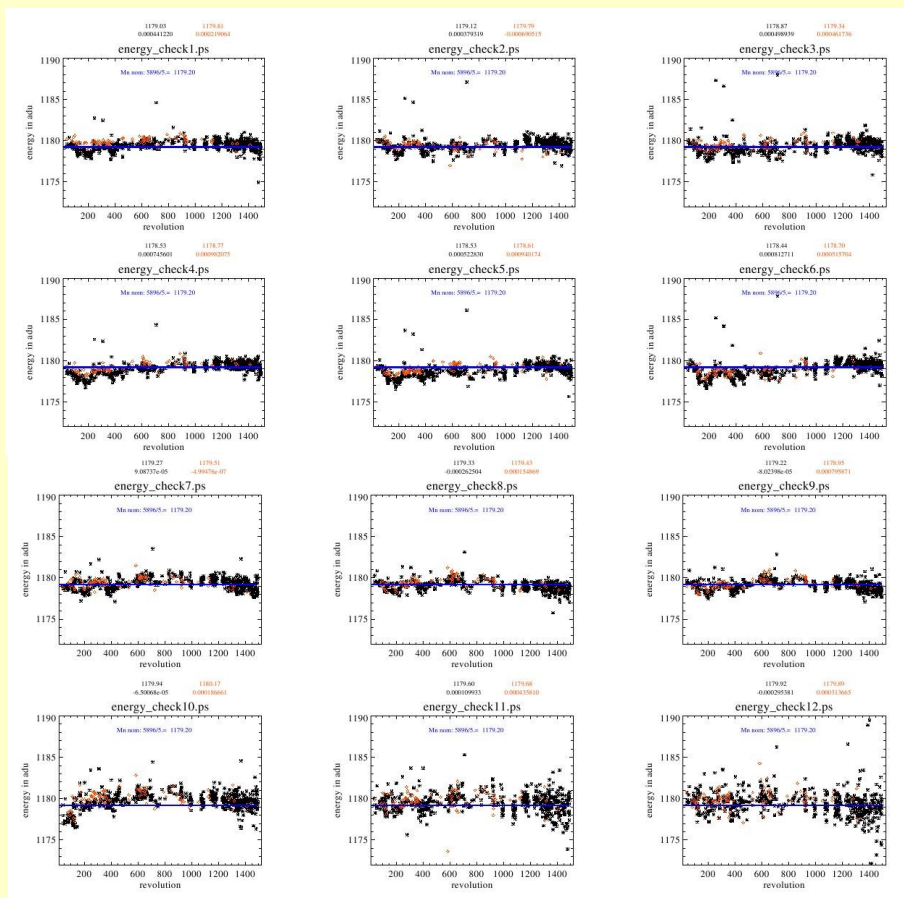
(Kirsch, Haberl, Dennerl, Freyberg 2007)

Temperature-dependent gain correction is the default as of SASv7.1.2



Refinement of CTI/gain

Refinement in pn long-term CTI

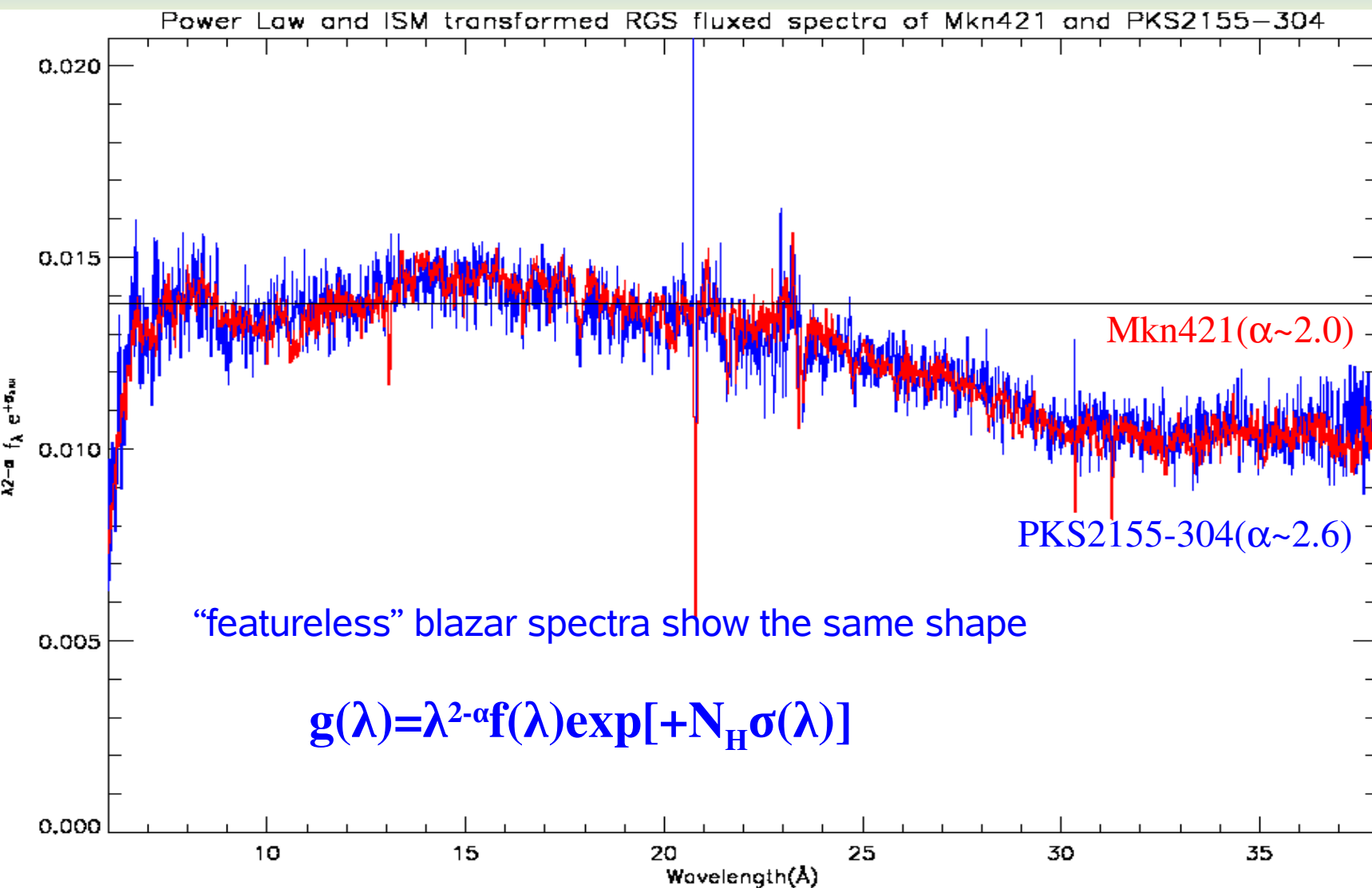


Additionally:

- Refinement of Timing Mode gain (astrophysically-based)
- Refinement of special CTI correction for pn Small Window (astrophysically-based)
- Refinement of CTI special correction for Large Window mode (PANTER measurement)



Basis of RGS effective-area corrections





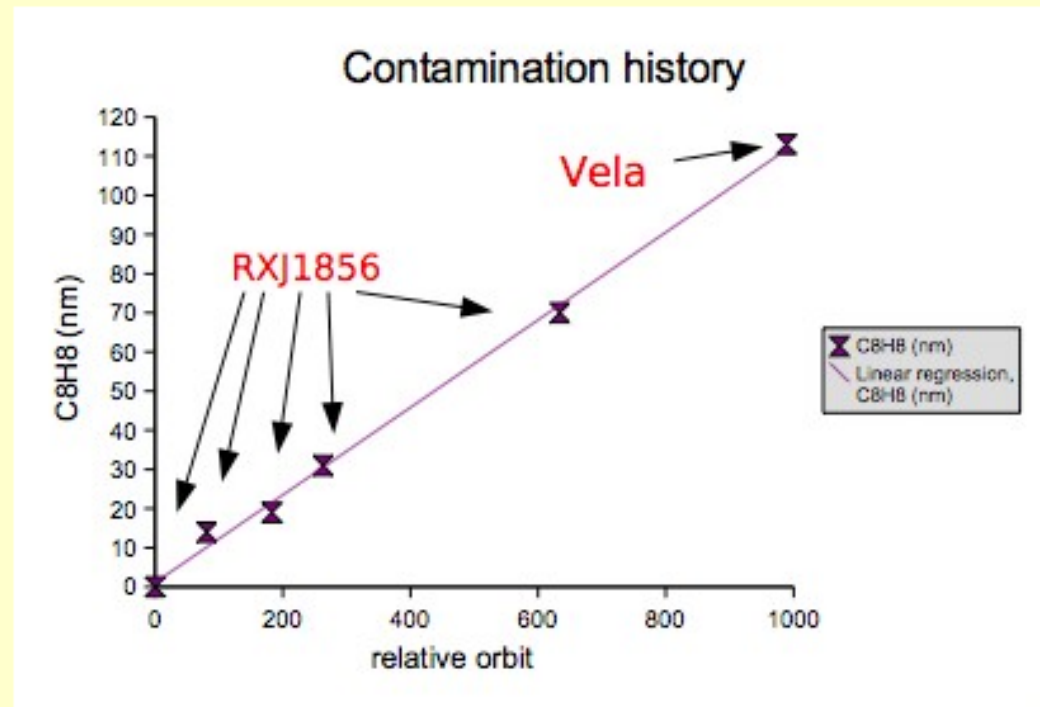
RGS effective-area corrections

- $\Delta(\text{RXJ1856-3754})$ & $\Delta(\text{Vela PWN})$
 - $\nabla \Rightarrow$ linear build-up of contamination by Carbon
- RGS EFFAREACORR CCF =
 - PolynomialCorrection(!t) \times exp(-Ct) \times CrabCorrection

Ex: [RXJ1856-3754 in RGS1](#)

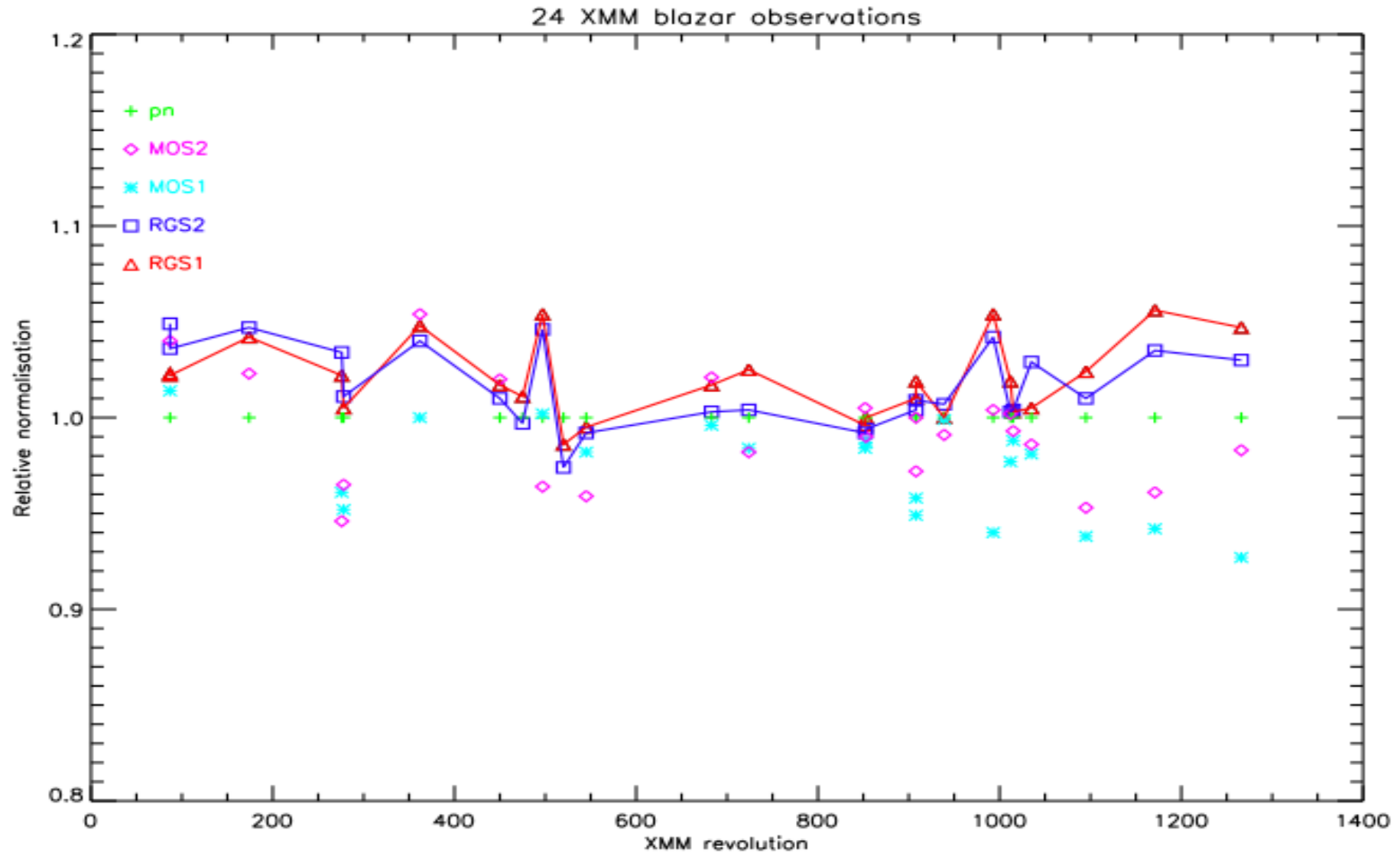
2002-04-08 : 0.171 ± 0.002 cts/s

2008-03-14: 0.147 ± 0.002 cts/s





RGS vs EPIC 2007-8 blazar statistics



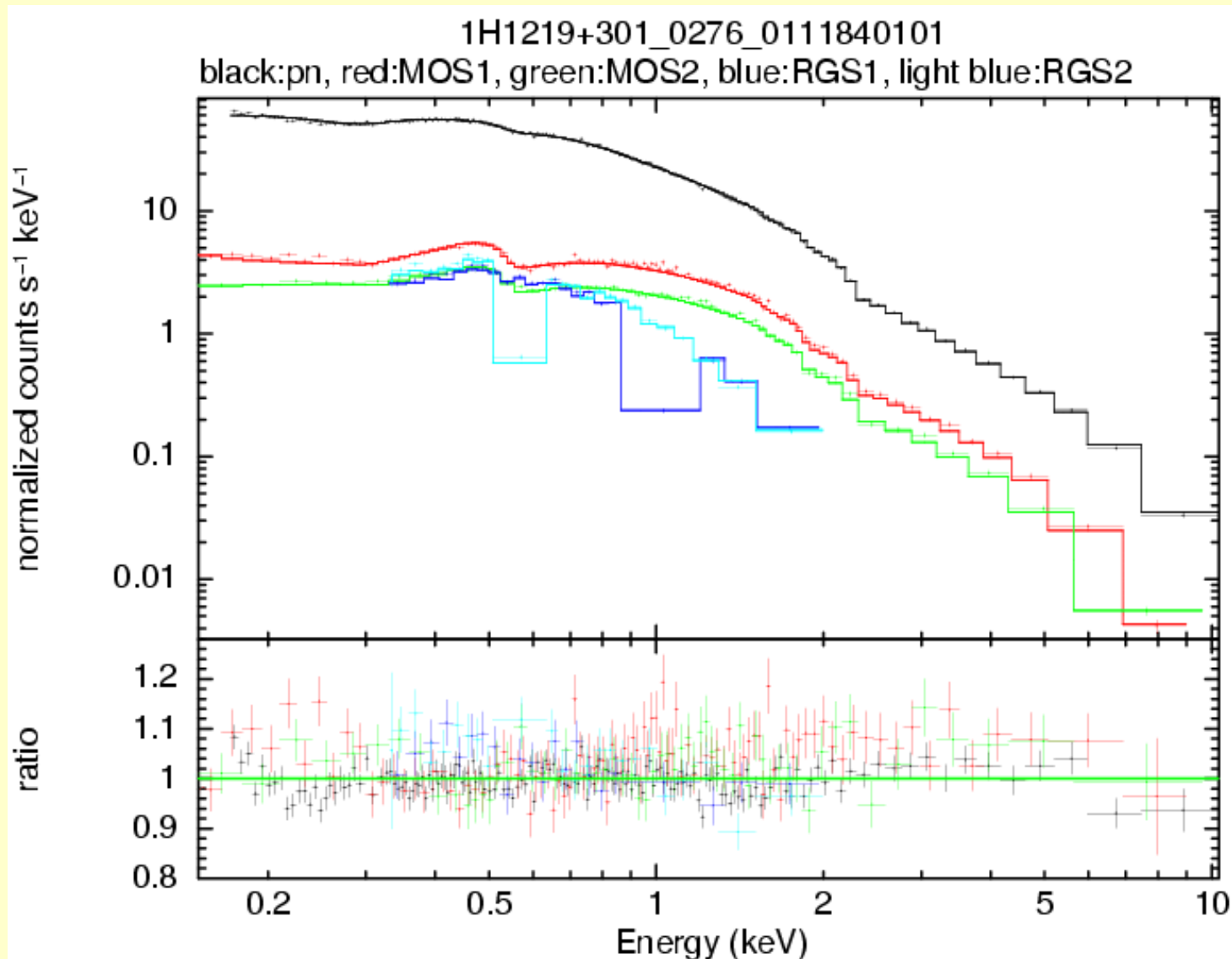


XMM-Newton cross-calibration archive

- 70 on-axis sources
- **NEW**: 24 off-axis sources (the brightest in the 2XMM catalog at off-axis angles i : $5' \leq i \leq 12'$)
- Spectral fitting examples on various sources using SASv7.1 and the public CCFs
 - Comparison with previous calibration/SAS versions possible
- Statistical evaluation of fluxes measured in 5 energy bands
- Evolution of spectral parameters as a function of time for multiple-observations sources
- Cross-calibration with *Chandra* and *Suzaku*:
 - *Chandra*: 3C273, Mkn421, Mkn590, PKS2155-304
 - *Suzaku*: PKS2155-204
- <http://xmm2.esac.esa.int/cgi-bin/ept/preview.pl?>

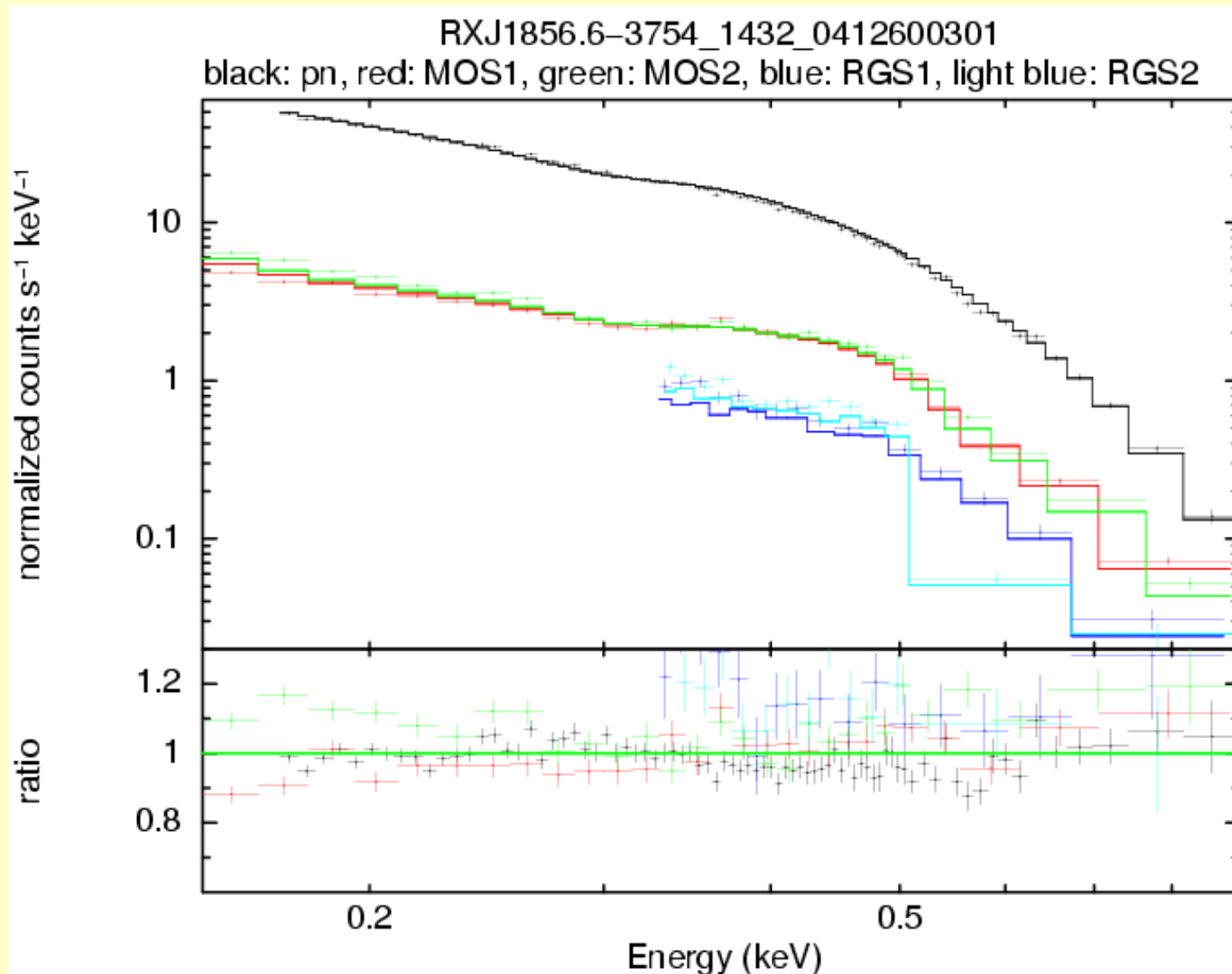


Representative examples: 1H1219+301



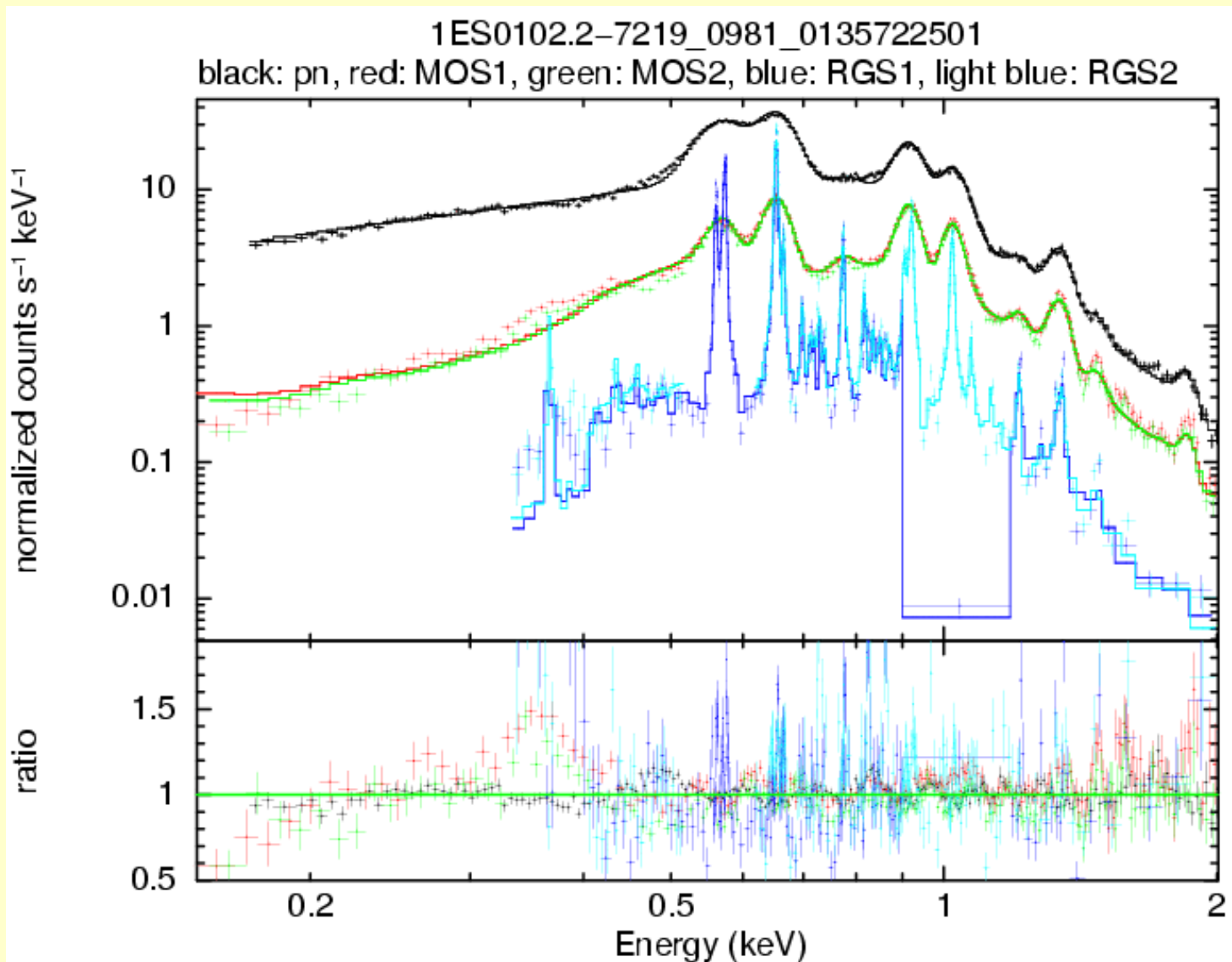


Low energy source: RXJ1856-3754





Line-rich source: 1ES0102-7219



- 39 lines
- 6 recombination edges
- absorbed bremsstrahlung
- joint fit to all instruments



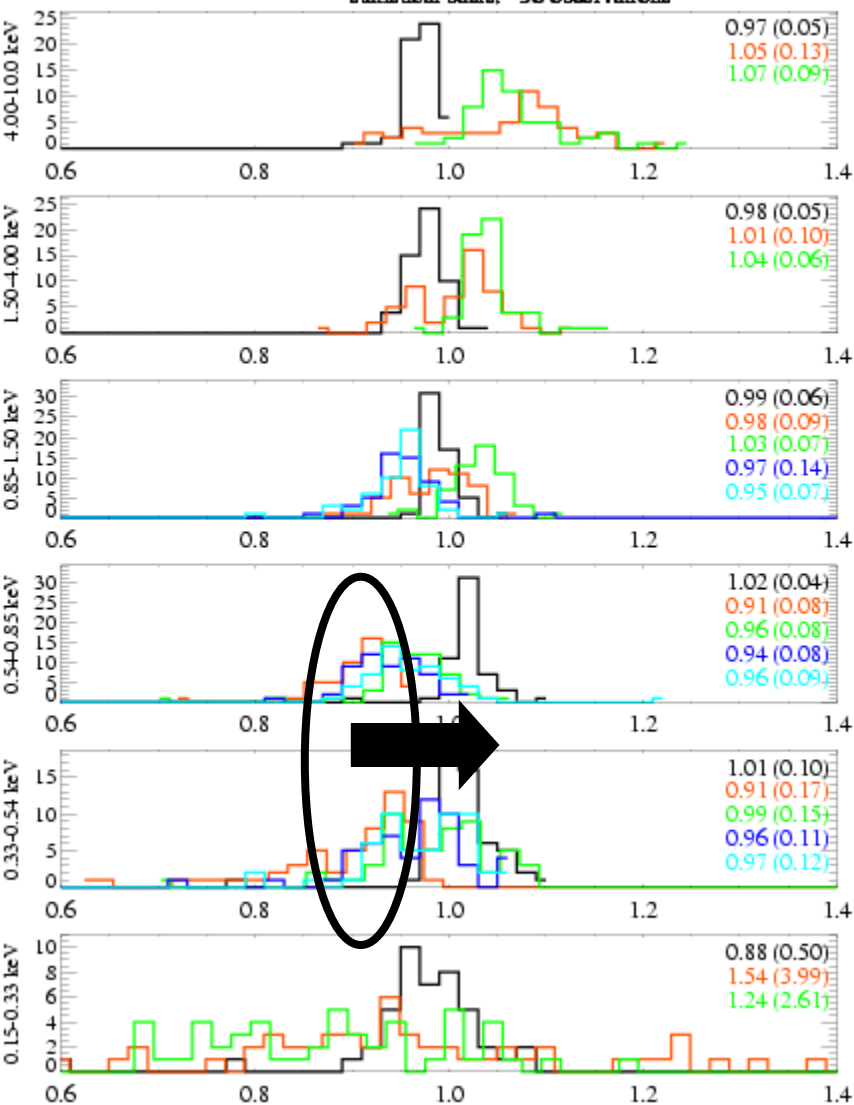
Statistical flux evaluation

SAS7.0

SAS7.1

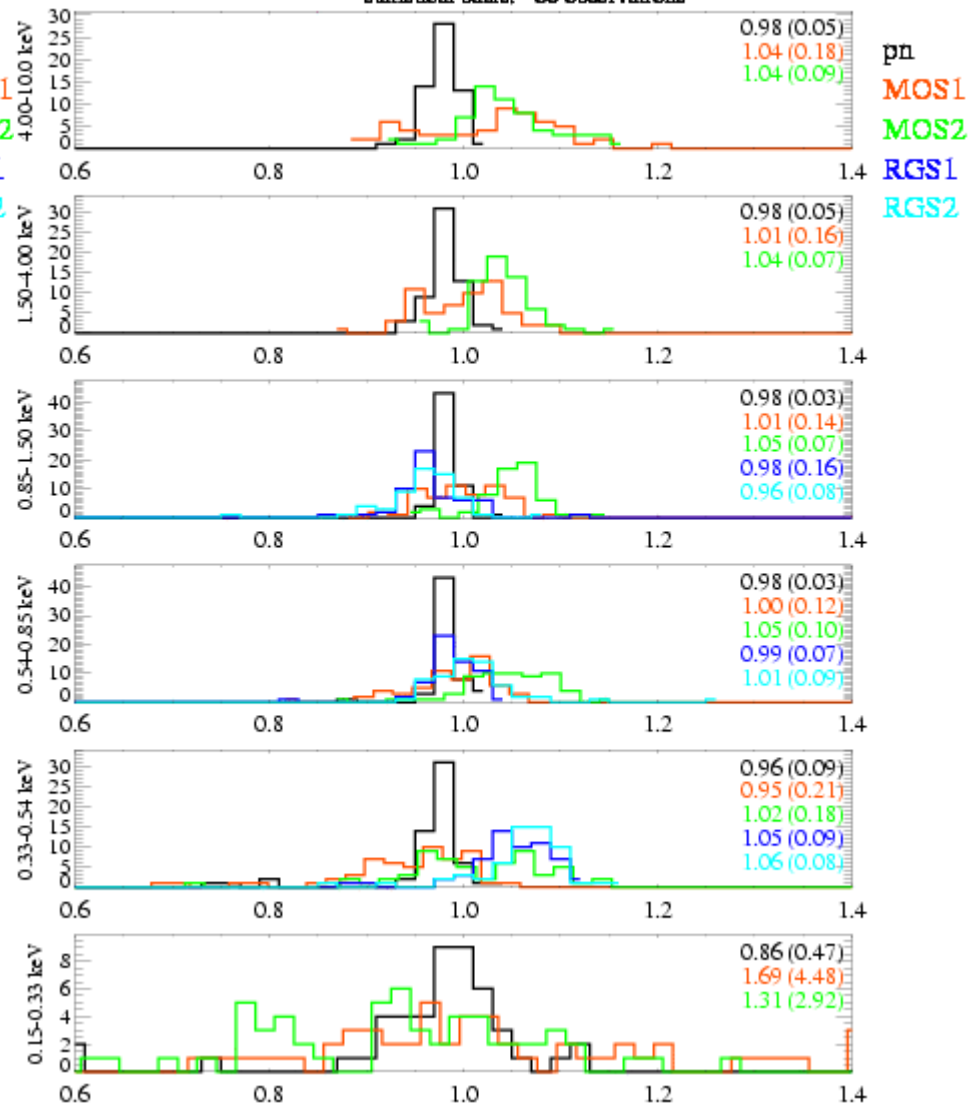
relative flux in different bands [Joint fit = 1]

statistical basis: 56 observations



relative flux in different bands [Joint fit = 1]

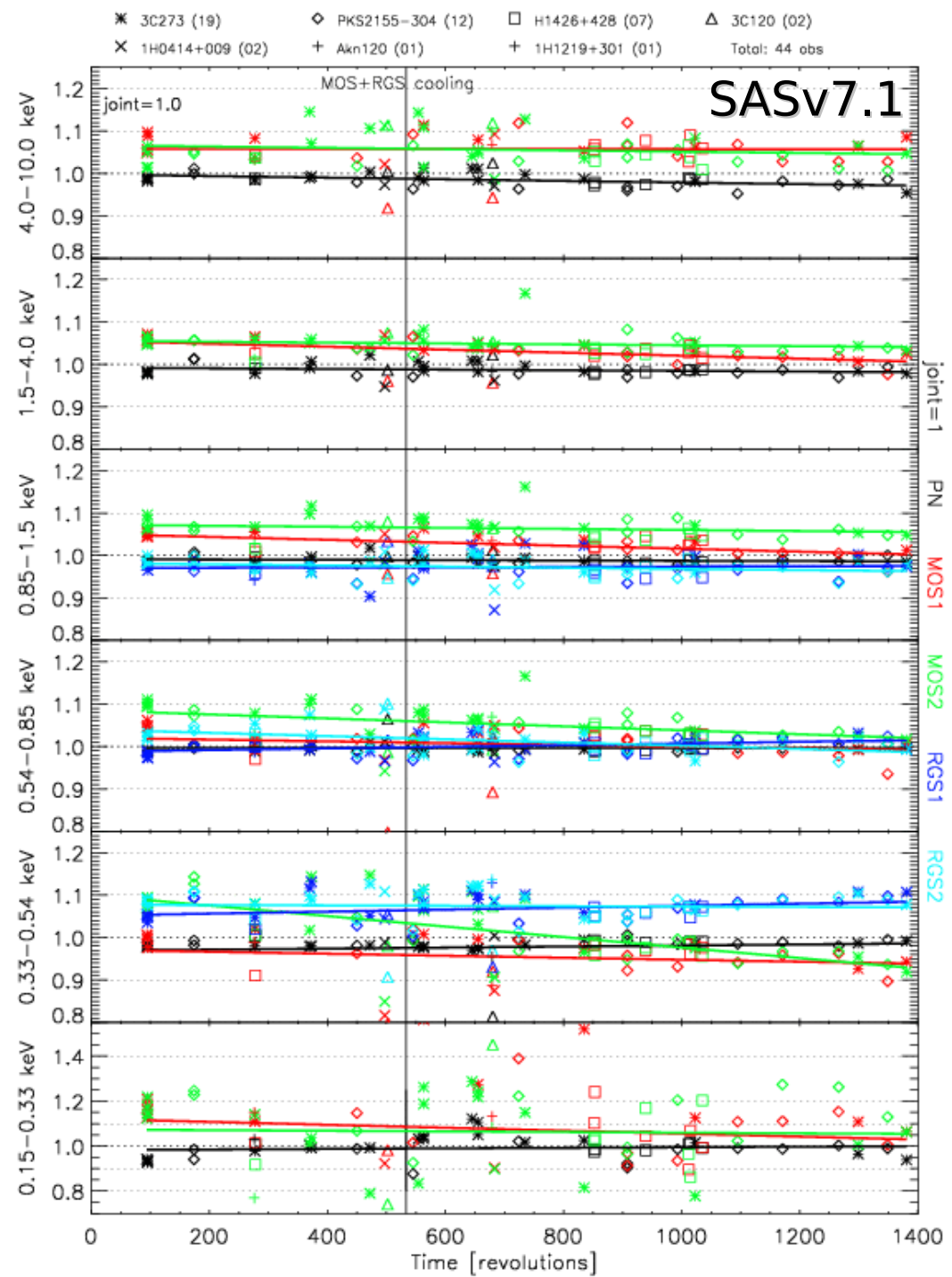
statistical basis: 60 observations



Flux ratio history

- Above ~ 0.8 keV, MOS fluxes are higher by on average 5-8% than pn.
- High deviations for MOS/pn flux ratios below 0.3 keV.
- Above O-edge RGS (up to 1.5 keV) and EPIC-pn agree to 2% on average.
- Below O-edge RGS fluxes are on average 5-10% higher than EPIC-pn.
- RGS flux ratios are stable for all energy bands.
- Possible trend with time in MOS/pn ratio being investigated

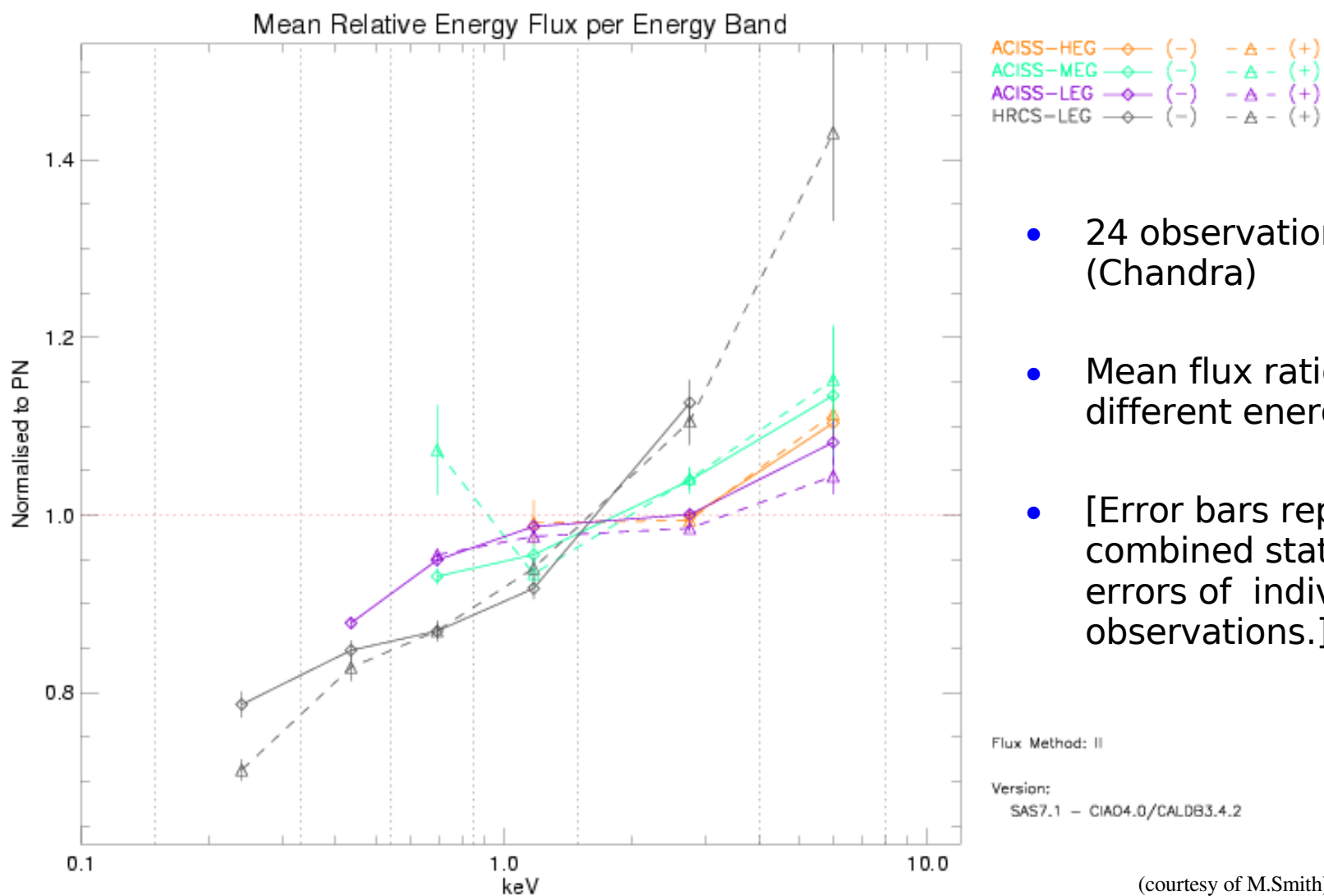
→ **EPIC and RGS are consistent on average within 10%.**





XMM-Newton/Chandra comparison

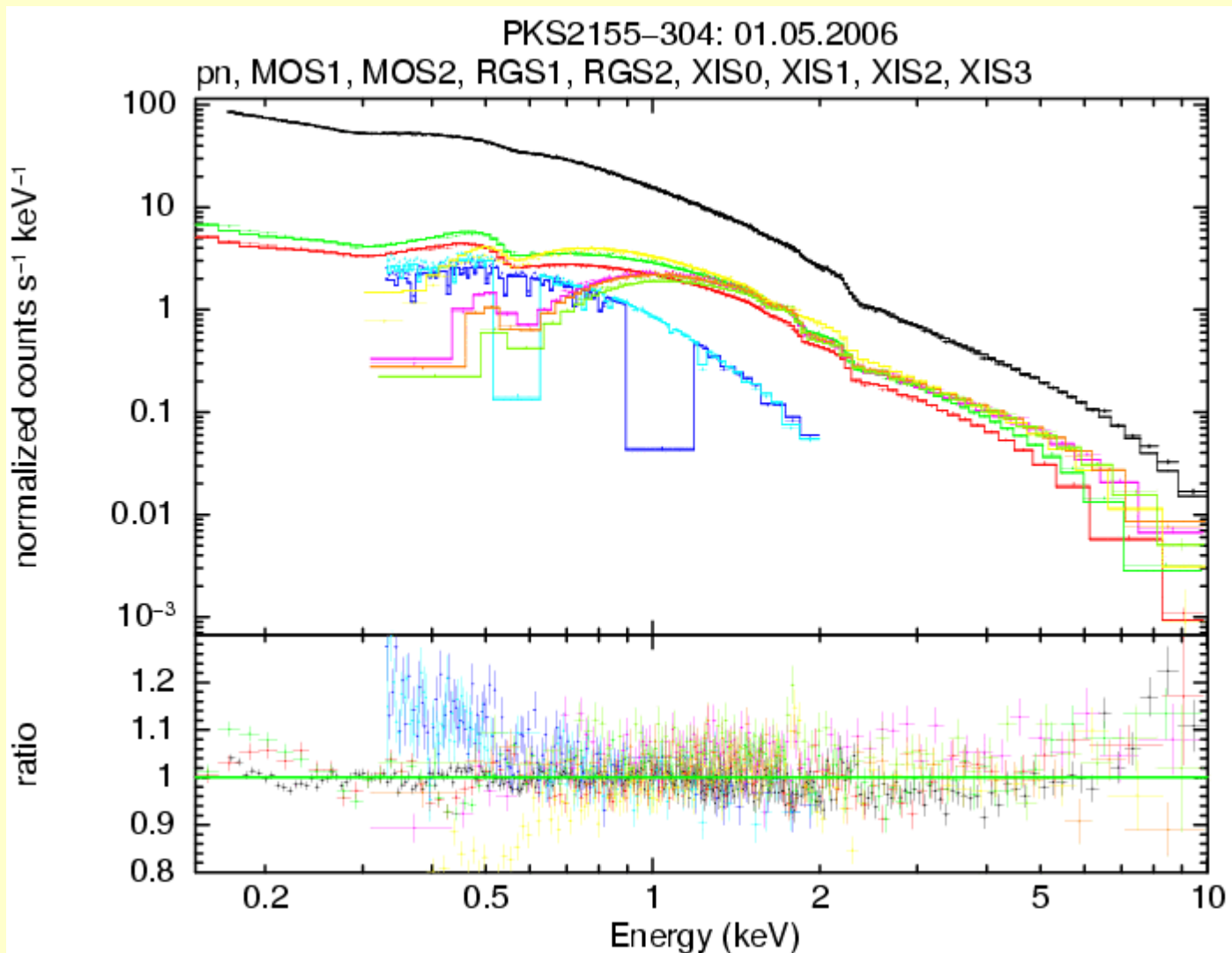
NEW: SOC XMM-Newton/Chandra cross-calibration archive





XMM-Newton versus Suzaku

NEW: SOC XMM-Newton/Suzaku cross-calibration archive

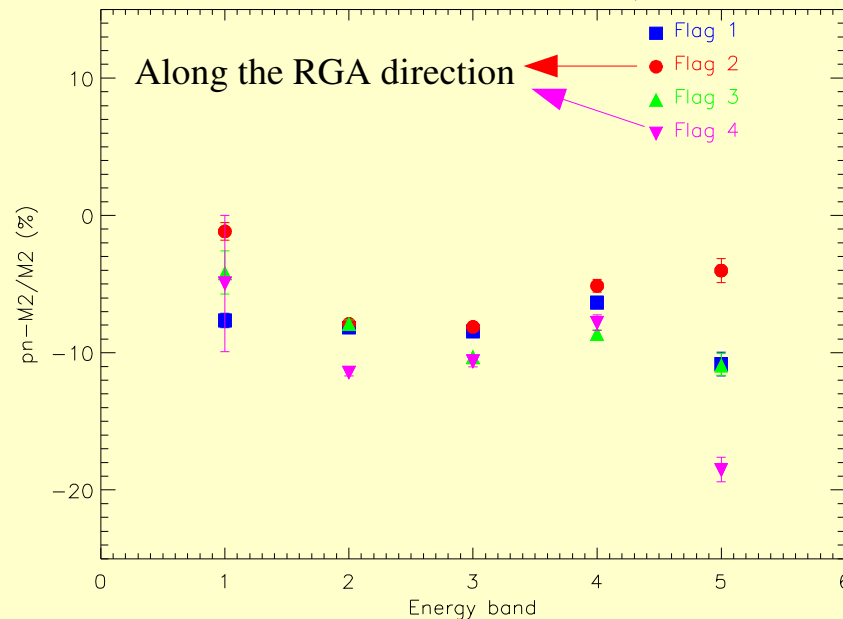
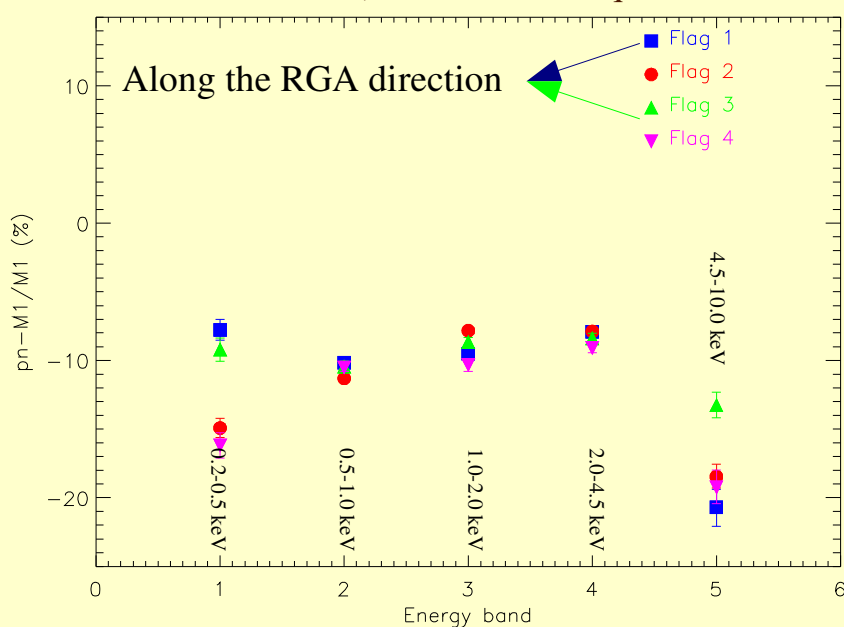


- PKS2155-304
- XMM rev. 1171
- FTOOLS 6.4
- Joint fit to all instruments.
- Absorbed single power law model
- $\chi^2_{\nu} = 1.36/10439$ dof
- Good general slope agreement.
- XIS fluxes slightly higher than EPICs.



Azimuth-dependence of camera fluxes in 2XMM

pn/MOS relative flux differences in 2XMM sources as a function of energy band
(colors code the quadrant in detector coordinates where the source is located)

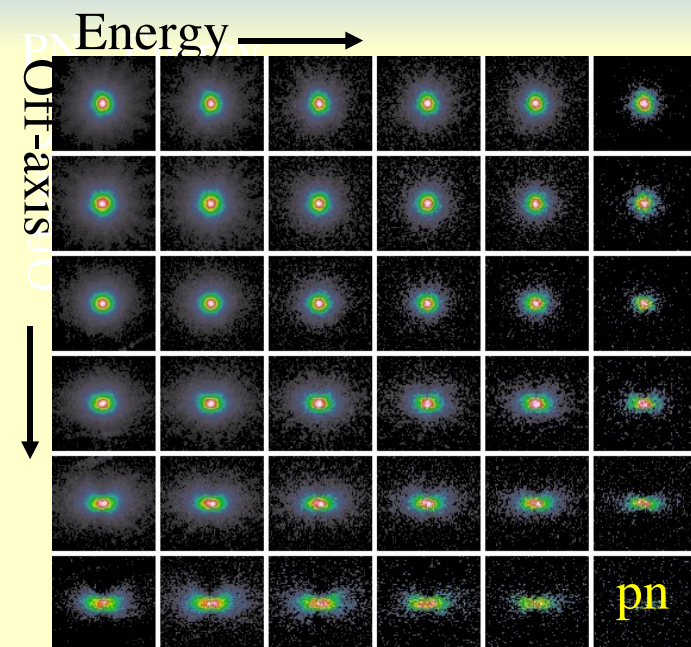


(Mateos et al. 2008)

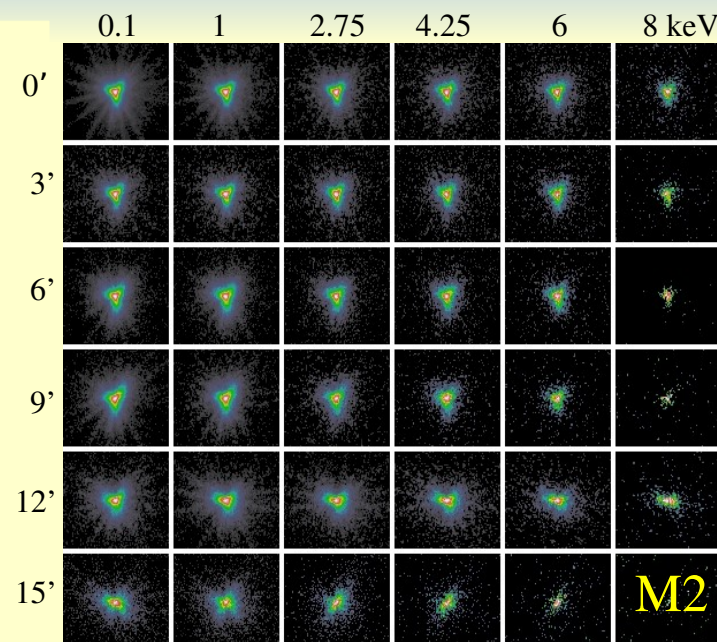
- In the 0.5-4.5 energy band average difference \cong 8-10%
- Azimuth-dependence of pn/MOS flux differences in the **4.5-12 keV** band
(spread in the **0.2-0.5 keV** band mostly due to the usage of a non-patch redistribution in 2XMM)



2-D parametrized EEF calculation



(courtesy of A.Read)



- Stacked images were fit with a “beta-model”: $\{A/[1+(r/r_0)^2]^\alpha\}$
- New CCF PSFs [ELLBETA] were generated with core radius, ellipticity, and power-law index as a function of camera, energy, off-axis
- SASv8.0 arfgen will use this “2-D PSF” to calculate the encircled energy fraction



EPIC calibration accuracy status

Effect	Max. Error	Energy dependent	Off axis angle dependent
Accuracy of the XMM-Newton frame with reference to optical frame	1''(r.m.s.)	NO	NO
Relative Astrometry	1.5''(r.m.s)	NO	YES
Absolute Astrometry	2.0''(r.m.s)	NO	YES
Point Spread Function (PSF)	2 %	YES	YES
Relative Effective Area	± 5 %	YES	YES
Absolute Effective Area	± 10 %	YES	YES
Absolute Energy scale	± 10 eV	YES	YES
Relative Timing	$\Delta P/P < 1E-8$	NO	NO
Absolute Timing	100 μ s	NO	NO



Cross-calibration status

- MOS flux above ~ 0.8 keV higher than pn by 5-8%.
- RGS and EPIC-pn flux ratios agree above O-edge to 2% on average.
- Current implementation of time-dependent RGS effective area model shows discrepancies below O-edge of 5-10%.
- RGS fluxes stable across the mission

EPIC and RGS are consistent on average within 10%.